

# Spatial distribution of superconducting and charge-density-wave order parameters in cuprates and its influence on the quasiparticle tunnel current (Review Article)

Alexander M. Gabovich and Alexander I. Voitenko

*Institute of Physics, National Academy of Sciences of Ukraine, 46 Nauka Ave., Kyiv 03680, Ukraine*

E-mail: gabovich@iop.kiev.ua,

voitenko@iop.kiev.ua

Received April 1, 2016, published online August 29, 2016

The state of the art concerning tunnel measurements of energy gaps in cuprate oxides has been analyzed. A detailed review of the relevant literature is made, and original results calculated for the quasiparticle tunnel current  $J(V)$  between a metallic tip and a disordered  $d$ -wave superconductor partially gapped by charge density waves (CDWs) are reported, because it is this model of high-temperature superconductors that becomes popular owing to recent experiments in which CDWs were observed directly. The current was calculated suggesting the scatter of both the superconducting and CDW order parameters due to the samples' intrinsic inhomogeneity. It was shown that peculiarities in the current-voltage characteristics inherent to the case of homogeneous superconducting material are severely smeared, and the CDW-related features transform into experimentally observed peak-dip-hump structures. Theoretical results were used to fit data measured for  $\text{YBa}_2\text{Cu}_3\text{O}_{7-\delta}$  and  $\text{Bi}_2\text{Sr}_2\text{CaCu}_2\text{O}_{8+\delta}$ . The fitting demonstrated a good qualitative agreement between the experiment and model calculations. The analysis of the energy gaps in high- $T_c$  superconductors is important both *per se* and as a tool to uncover the nature of superconductivity in cuprates not elucidated so far despite of much theoretical effort and experimental progress.

PACS: 71.45.Lr Charge-density-wave systems;

74.55.+v Tunneling phenomena: single particle tunneling and STM;

74.81.-g Inhomogeneous superconductors and superconducting systems, including electronic inhomogeneities.

Keywords:  $d$ -wave superconductivity, charge-density wave, quasiparticle tunnel spectrum, peak-dip-hump structure, pseudogap, high- $T_c$  superconductor.

## Contents

1. High- $T_c$ superconductors and charge-density waves .....	1103
2. Theoretical basis.....	1106
3. Quasiparticle current.....	1107
4. Account of inhomogeneity .....	1108
5. Conductance-voltage characteristics. Background problem.....	1109
6. Results of calculations and discussion .....	1110
7. Conclusions.....	1111
References.....	1111

## 1. High- $T_c$ superconductors and charge-density waves

Superconductivity of high- $T_c$  oxides is a vast area of materials science [1]. Nevertheless, although about thirty years passed since this phenomenon had been discovered,

it remains unexplained so far from a microscopic point of view [2–6]. The lack of explanation means that we still do not know for sure what boson (bosons) is responsible for the Cooper pairing, although the Bardeen–Cooper–Schrieffer (BCS) character of superconductivity (in the

broad sense of this term [7]) is beyond question. Anyway, the absence of the knowledge on the “glue” between paired electrons does not allow one to predict and precisely calculate the critical temperature of superconducting transition,  $T_c$ , or any other important critical parameter [8]. Only rare accidental success happens sometimes [9,10], which might be simply a stroke of luck. One of the problems impeding the exact solution of the basic Eliashberg equations (for the electron-phonon or other mechanisms of superconductivity [11]) is the ubiquitous and ambiguous Coulomb pseudopotential [11].

Another problem arising while making attempts to carry out reliable calculations of superconducting properties is the proper account of strong electron-electron correlations, which, in principle, may even dominate in the normal-state and superconducting behavior of perspective materials [12,13]. Many-body correlations can lead to other competing electron-spectrum instabilities different from Cooper pairing. In particular, these are charge density waves (CDWs), which distort the nested Fermi surface (FS) sections by the emergence of dielectric energy gaps [14,15]. Experiments show that CDWs do appear in cuprates [16–24] and the intertwining between the CDW and superconducting gappings is a hot issue of condensed matter physics [25–30]. It has to be indicated that cuprates also host the so-called pseudogaps [31,32], which we identify as CDW related gaps. Nevertheless, it might also happen that the both phenomena are interrelated, but not identical.

The existence of intrinsic disorder in high- $T_c$  oxides is another factor, which makes the identification of CDW gaps more complicated than that of their superconducting counterparts [33–38] as comes about from the scanning-tunnel-microscopy (STM) measurements. The spread of the latter over the sample surface is also quite wide, although the distribution histogram for the superconducting gaps is narrower than that for the CDW ones in the cases when the both kinds can be distinguished [39]. Examples of such histograms taken from Refs. 40–49 are shown in Fig. 1.

We would like to attract attention to the variety of gap distributions. In particular, the superconductivity- and CDW-driven gap histograms can be either strongly overlapped or well separated. Concerning the latter case (see Fig. 1, panels (c) and (j)–(l)), it should be emphasized that, in the framework of our model (see Sec. 2), the smaller-gap clusters are associated with the distributions of a pure  $d$ -wave superconducting gap, whereas the larger-gap ones with those of a combined (superconducting + CDW) gap. However, near  $T_c$  (see panels (d) and (e)), the distribution is governed predominately (below  $T_c$ ) or exclusively (above  $T_c$ ) by the spread of CDW strength.

The reasons of the electronic inhomogeneity leading to the inhomogeneous electron-spectrum gapping may be different, with the oxygen non-stoichiometry [50] being an infeasible factor for cuprates [51]. Both CDWs and the

electronic nonhomogeneity should be crucial for tunnel spectroscopy, which studies voltage,  $V$ , dependences of the quasiparticle current  $J$  and the corresponding conductance  $G(V) = dJ/dV$  [52–56]. Some time ago we suggested that CDWs have already been detected in the quasiparticle tunnel current-voltage characteristics [30,57–60]. Specifically,  $G(V)$  of junctions (either symmetric or non-symmetric ones) involving high- $T_c$  oxides reveal peak-dip-hump structures at energies  $eV$  much larger than the superconducting gap-edge positions  $\Delta$  [25,31,55,61,62]. Here,  $e > 0$  is the elementary electric charge.

There are other scenarios, alternative to our approach (see references in our publications [30,60]), which attempt to explain the existence of those structures. Their main difficulty consists in inevitable conspicuous CDW traces in tunnel junctions with cuprate electrodes; such traces were earlier observed in a number of partially CDW-gapped normal metals and superconductors [63–65]. This phenomenon is a simple consequence of the dielectric gap emergence on FS sections, which is similar to the superconducting gapping, because the coherence factors disappear from the expression for  $J(V)$  [66]. That is why the basic model of the quasiparticle tunneling between superconductors is called a “semiconductor” one. Hence, the CDW manifestations should be at least as strong as superconducting ones. One can see that this is the case with the temperature above  $T_c$ , when the pseudogap-induced depletion in the density of states is easily detected [31,55,67,68]. The evidence is not so clear for temperatures below  $T_c$ , since one observes either weak peak-dip-hump structures mentioned above (and discussed in more detail in following sections) or co-existing distinct CDW- and superconductivity-driven gap-edge peaks [69,70]. The latter interpretation was however questioned [71], because heating effects might spoil the picture (see also the earlier work [72] dealing with  $\text{BaPb}_{1-x}\text{Bi}_x\text{O}_3$  ceramics, the predecessor of high- $T_c$  oxides).

The observed CDW structures in cuprates are not so pronounced as, say, their counterparts in tri- [63,65,73] or dichalcogenides [63,74–76]. The indicated disorder leading to the spatial averaging of CDW manifestations is one of the reasons. An underdevelopment of superlattice structure, i.e., its short-range or fluctuating CDW character [17,77–79] in high- $T_c$  oxides may be another reason of its apparent suppression in tunnel measurements. The weakness of CDW distortions, accompanied by fluctuations, and the smallness of CDW domains may be intimately connected to disorder [80]. This fact makes the elaboration of adequate microscopic theories rather involved.

Moreover, one should point at the commonly occurring four-fold  $C_4$  symmetry loss of the reconstructed cuprate two-dimensional electron spectrum. As a result, there emerges the  $C_2$  (nematic or smectic) charge order, which has already been found not only in high- $T_c$  oxides but also in iron-based superconductors [22,81–86]. The relevant experiments for cuprates demonstrate that the symmetry

violation is not mandatory. Therefore, both bidirectional (checkerboard) CDWs, which preserve the  $C_4$  symmetry, and unidirectional (stripe) patterns corresponding to ne-

matic or smectic states are possible. Hence, they should be considered while studying tunnel currents in junctions made of CDW superconductors.

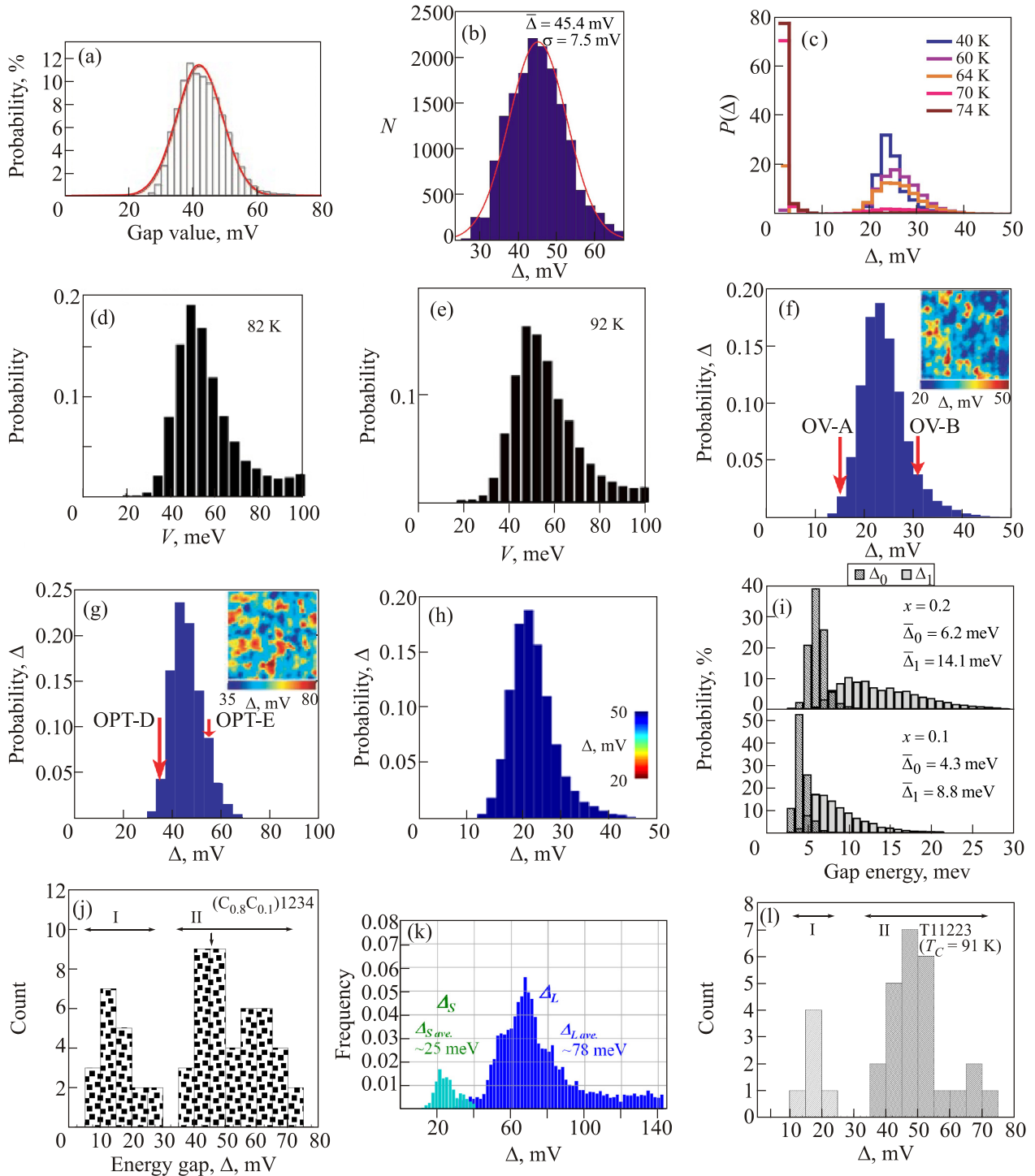


**Fig. 1.** (Color online) Histograms of energy-gap distributions in various cuprates revealed by scanning tunnel microscopy (STM) experiments: (a) overdoped  $\text{Bi}_2\text{Sr}_2\text{CaCu}_2\text{O}_{8+\delta}$  (BSCCO), the critical temperature  $T_c = 84$  K [40]; (b) overdoped BSCCO,  $T_c = 86\text{--}87$  K [41]; (c) overdoped BSCCO,  $T_c = 65$  K, measured at various temperatures  $T$ 's [42]; (d) underdoped BSCCO,  $T_c = 87$  K, measured at  $T = 82$  K [43]; (e) underdoped BSCCO,  $T_c = 87$  K, measured at  $T = 92$  K [43]; (f) overdoped BSCCO,  $T_c = 68$  K [44]; (g) optimally doped BSCCO,  $T_c = 93$  K [44]; (h) overdoped BSCCO,  $T_c = 68$  K [45]; (i) overdoped  $\text{Bi}_2\text{Sr}_{2-x}\text{La}_x\text{CuO}_{6+\delta}$ , (bottom)  $x = 0.1$ ,  $T_c = 14$  K; (top)  $x = 0.2$ ,  $T_c = 31$  K [46]; (j)  $(\text{Cu,C})\text{Ba}_2\text{Ca}_3\text{Cu}_4\text{O}_{12+\delta}$ ,  $T_c = 117$  K [47]; (k)  $\text{Ba}_2\text{Ca}_4\text{Cu}_5\text{O}_{10}(\text{O}_{0.17}\text{F}_{0.83})_2$ ,  $T_c = 70$  K [48]; (l)  $\text{TlBa}_2\text{Ca}_2\text{Cu}_2\text{O}_{10-\delta}$ ,  $T_c = 91$  K [49].

## 2. Theoretical basis

The idea that the electron spectrum peculiarities of high- $T_c$  oxides can be associated with the existence of CDWs was put forward by us not long ago after the cuprates had been discovered [87,88]. For  $d$ -wave superconductors with  $s$ -wave CDWs, we use a theoretical framework suggested earlier [25,27,60,89]. This treatment, in agreement with the experimental data for cuprates, assumes a  $d_{x^2-y^2}$ -wave BCS-like superconducting order parameter and an  $s$ -wave CDW order parameter attributed to certain (nested) FS sections at temperatures below the critical one,  $T_s$ , which is usually substantially higher than  $T_c$ . This includes  $N = 4$  (bidirectional CDWs) or 2 (unidirectional CDWs) sectors.

The mean-field Hamiltonian has the form

$$H = H_{\text{kin}} + H_{\text{BCS}} + H_{\text{CDW}}, \quad (1)$$

where

$$H_{\text{kin}} = \sum_{\mathbf{k}, \sigma=\uparrow, \downarrow} \xi_i(\mathbf{k}) a_{i, \mathbf{k}, \sigma}^\dagger a_{i, \mathbf{k}, \sigma}, \quad (2)$$

$$H_{\text{BCS}} = \sum_{\mathbf{k}} \bar{\Delta}(\mathbf{k}) \sum_{i=d, nd} a_{i, \mathbf{k}, \uparrow}^\dagger a_{i, -\mathbf{k}, \downarrow}^\dagger + \text{c.c.}, \quad (3)$$

$$H_{\text{CDW}} = \sum_{\mathbf{k}, \sigma=\uparrow, \downarrow} \sum_{i=d} \bar{\Sigma}(\mathbf{k}) a_{i, \mathbf{k}, \sigma}^\dagger a_{i, \mathbf{k}+\mathbf{Q}, \sigma} + \text{c.c.} \quad (4)$$

Here,  $\xi_i(\mathbf{k})$  is the initial quasiparticle spectrum; the  $d$ -wave superconducting momentum-dependent order parameter,  $\bar{\Delta}(\mathbf{k})$ , and the  $s$ -wave dielectric one,  $\bar{\Sigma}(\mathbf{k})$ , are described below;  $a^\dagger$  and  $a$  are the creation and annihilation operators, respectively;  $\sigma$  is the quasiparticle spin projection,  $\mathbf{Q}$  is the CDW vector, and the notations “ $d$ ” and “ $nd$ ” indicate the CDW-gapped or in other words dielectrized (to distinguish this pairing mechanism from the superconducting one, we will use hereafter the term “dielectrized”) and non-dielectrized FS sections, respectively.

In the parent non-superconducting CDW state, the  $s$ -wave-like CDW (dielectric) complex order parameter  $\Sigma_0(T) e^{i\varphi}$  (here,  $\varphi$  is the CDW phase) is constant within any of  $N$  dielectrized sectors directed along the  $\mathbf{k}_x$  and  $\mathbf{k}_y$  axes (see Fig. 2). Each of the sectors spans the angle  $2\alpha < \Omega$  ( $\Omega = 90^\circ$  for  $N = 4$  or  $180^\circ$  for  $N = 2$ ); this is the model of partial FS dielectrization. In the adopted  $s$ -wave theory [14,90,91], the zero-temperature magnitude of CDW order parameter equals  $\Sigma_0(T=0) = (\pi/\gamma)T_{s0}$ , where  $\gamma = 1.78\dots$  is the Euler constant, the Boltzmann constant  $k_B = 1$ , and  $T_{s0} = T_s$  since there is no influence of  $\Delta$  in the normal state. The CDW order parameter itself has the conventional  $s$ -wave dependence on  $T$ ,

$$\Sigma_0(T) = \Sigma_0(0) \text{Mü}_s(T/T_{s0}), \quad (5)$$

where  $\text{Mü}_s(x)$  is the reduced [ $\text{Mü}_s(0) = 1$ ]  $s$ -Mühschlegel function. The angle  $\theta$  in the two-dimensional  $\mathbf{k}$ -plane is

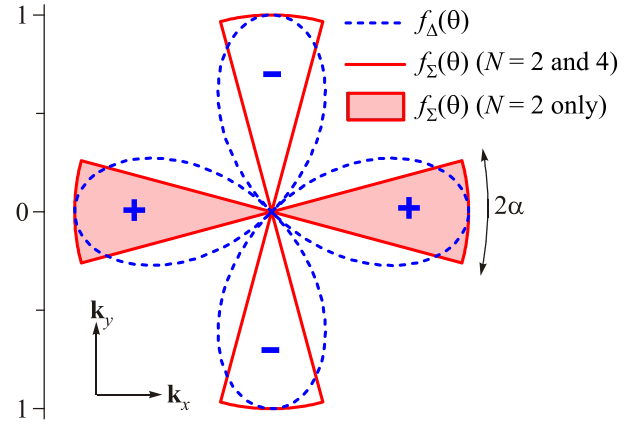


Fig. 2. (Color online) Angular factors of order parameters for the partially gapped CDW  $d$ -wave superconductor.

reckoned from the  $\mathbf{k}_x$  axis. The profile  $\bar{\Sigma}_0(T, \mathbf{k})$ , or  $\bar{\Sigma}_0(T, \theta)$ , over the whole FS contains the factor  $f_\Sigma(\theta)$ , which is equal to 1 inside each dielectrized sector and 0 otherwise (see Fig. 2), so that

$$\bar{\Sigma}_0(T, \theta) = \Sigma_0(T) f_\Sigma(\theta). \quad (6)$$

The parent non-dielectrized BCS  $d_{x^2-y^2}$ -wave superconductor (dBCS) [92] is characterized by the superconducting order parameter  $\Delta_0(0)$  at  $T = 0$  and  $T_{c0} = (\gamma\sqrt{e}/2\pi)\Delta_0(0)$ , where  $e$  is the base of natural logarithm. The order parameter lobes are oriented in the  $\mathbf{k}_x$  and  $\mathbf{k}_y$  directions, i.e., in the same (antinode) directions as the bisectrices of CDW sectors. The profile  $\bar{\Delta}_0(T, \theta)$  in the  $\mathbf{k}$ -space spans the whole FS

$$\bar{\Delta}_0(T, \theta) = \Delta_0(T) f_\Delta(\theta), \quad (7)$$

where (see Fig. 2)

$$f_\Delta(\theta) = \cos 2\theta \quad (8)$$

and

$$\Delta_0(T) = \Delta_0(0) \text{Mü}_d(T/T_{c0}). \quad (9)$$

Here,  $\text{Mü}_d(x)$  is the conventional  $d$ -wave superconducting order parameter dependence.

When CDWs and superconductivity coexist (we call this state SCDW), the order parameter dependences  $\Sigma(T)$  and  $\Delta(T)$  differ from those of the pure phases, i.e.,  $\Sigma_0(T)$  and  $\Delta_0(T)$ , respectively [26,27]. The resulting self-consistent set of gap equations, which determines  $\Sigma(T)$  and  $\Delta(T)$  for the given set of the input model parameters ( $\Delta_0(0)$ ,  $\Sigma_0(0)$  — for brevity, they are denoted below as  $\Delta_0$  and  $\Sigma_0$ , respectively —  $\alpha$ , and  $N$ ) has the following form obtained earlier [25–27,30]:

$$\int_{-\alpha}^{\alpha} I_M(\sqrt{\Sigma^2 + \Delta^2 \cos^2 2\theta}, T, \Sigma_0) d\theta = 0, \quad (10)$$

$$\int_{-\alpha}^{\alpha} I_M(\sqrt{\Sigma^2 + \Delta^2} \cos^2 2\theta, T, \Delta_0 \cos 2\theta) \cos^2 2\theta d\theta + \int_{\alpha}^{\Omega-\alpha} I_M(\Delta \cos 2\theta, T, \Delta_0 \cos 2\theta) \cos^2 2\theta d\theta = 0, \quad (11)$$

here

$$I_M(\Delta, T, \Delta_0) = \int_0^{\infty} \left( \frac{1}{\sqrt{\xi^2 + \Delta^2}} \tanh \frac{\sqrt{\xi^2 + \Delta^2}}{2T} - \frac{1}{\sqrt{\xi^2 + \Delta_0^2}} \right) d\xi \quad (12)$$

is the Mühlshlegel integral of the BCS theory. Due to the order parameter interplay, the lowest of the initial temperatures  $T_{c0}$  or  $T_{s0}$  is suppressed due to the competition, so that the actual critical temperatures become  $T_c < T_{c0}$  or  $T_s < T_{s0}$ . For existing CDW superconductors, it was found that  $T_c < T_s$  [14,25,65].

The overall gap on the whole FS (the gap rose) can be written in the form

$$\bar{D}(T, \theta) = \sqrt{\bar{\Sigma}^2(T, \theta) + \bar{\Delta}^2(T, \theta)}, \quad (13)$$

where

$$\bar{\Delta}(T, \theta) = \Delta(T) f_{\Delta}(\theta), \quad (14)$$

$$\bar{\Sigma}(T, \theta) = \Sigma(T) f_{\Sigma}(\theta). \quad (15)$$

In other words, in the mixed phase, a combined gap

$$\bar{D}(T, \theta) = \sqrt{\bar{\Sigma}^2(T) + \bar{\Delta}^2(T, \theta)}$$

determined by both order parameters, appears on the  $d$  FS sections, and the gap  $|\bar{\Delta}(T, \theta)|$  depending only on the superconducting order parameter exists on the  $nd$  ones.

### 3. Quasiparticle current

In the framework of general approach, we consider quasiparticle tunneling along the  $c$ -axes of both SCDW electrodes, i.e., between the superconducting planes of the same crystal or between two cuprate crystals, which are suggested to be partially CDW-gapped  $d$ -wave SCDWs with their superconducting planes ( $a$ - $b$  facets) oriented parallel to the junction interface. Such a configuration can be realized in mesas [93,94], twist-crystal structures made of bicrystals [95], the artificial cross-whiskers [96], or the natural cross-whiskers [97]. We assume the strongly incoherent tunneling in the  $c$ -direction between electrodes supported by the experimental evidence for the Josephson current [98]. However, the opposite case of the  $c$ -axis coherent tunneling would give similar results.

The formulas for the current  $J(V)$  through the junction concerned were obtained in the tunnel-Hamiltonian approach [14,57,99–103]

$$J(V) = \frac{1}{2(2\pi)^2 eR} \int_{-\pi}^{\pi} d\theta \int_{-\pi}^{\pi} d\theta' \int_{-\infty}^{\infty} d\omega \times K(\omega, V, T) P(\omega, \theta) P'(\omega - eV, \theta'), \quad (16)$$

where

$$K(\omega, V, T) = \tanh \frac{\omega}{2T} - \tanh \frac{\omega - eV}{2T}; \quad (17)$$

and the  $P$ -factors describe SCDW electrodes. All the tunnel barrier properties were incorporated into the single constant  $R$  describing the normal-state resistance. The primed quantities are associated with the electrode that the potential  $V$  is applied to (the  $V$ -electrode); its counter electrode will be referred to as 0-electrode. In particular, for the 0-electrode,

$$P(\omega, \theta) = \frac{\Theta(|\omega| - \bar{D}(T, \theta))}{\sqrt{\omega^2 - \bar{D}^2(T, \theta)}} \times [|\omega| + \text{sign } \omega \cos \varphi \bar{\Sigma}(T, \theta)], \quad (18)$$

where  $\Theta(x)$  is the Heaviside step-function, the CDW phase  $\varphi$  is usually pinned by the junction interface and acquires the values 0 or  $\pi$  (see discussion in Refs. 14, 25). For  $P'(\omega - eV, \theta')$ , one has  $\omega - eV$  rather than  $\omega$  in formula (18), whereas all other parameters have to be primed, i.e., associated with the  $V$ -electrode. The peculiar term in the brackets of Eq. (18) is generated by the electron-hole-pairing Green's function  $G_{ib}$ , which is dubbed “normal” because it is proportional to the product  $c_l^\dagger c_r$  [104,105]. However, this term can also be called “anomalous”, since it contains the CDW order parameter as a factor, in the same way as the Gor'kov Green's function  $F$  is proportional to the factor  $\Delta$  [99]. Here, the subscripts  $l$  and  $r$  correspond to two different nested FS sections.

If one of the electrodes is a normal metal we arrive at a specific junction variant, which is typical of STM studies of the quasiparticle tunnel current between the tip and the superconducting cuprate plane (the STM configuration). In this case, the  $P(\omega, \theta)$  function corresponding to the normal metal becomes identical to unity and drops out of consideration. Below, we will make specific calculations just for this case (although, in principle, the symmetric one is not more difficult for studying). In the case of non-symmetric configuration, the CVC is non-symmetric [106] in accordance with  $G(V)$ 's observed for high- $T_c$  superconductors [55,56,107].

We emphasize that the appearance of the dielectric gap  $\Sigma$  in expression (16) for the tunnel current is justified by the same arguments as the now-conventional emergence of its superconducting counterpart  $\Delta$ . The problem of the collective-state-gap manifestations started with the Harrison's analysis [108] carried out in the framework of the independent-particle picture and using quite a reasonable Wentzel–Kramers–Brillouin approximation [109]. This author show-



ed that in the one-dimensional case the density-of-states factor should be canceled out from the final expression for the tunnel current due to the dependence of the tunneling matrix element  $T_{12}$  on this factor [108]. As was demonstrated experimentally by Giaever [110,111], this approach fails in the case of quasiparticle tunneling between superconductors or between a normal metal and a superconductor, because many-body correlations enter into the game. Thus, the tunnel current becomes a functional of the so-called superconducting densities of states, which are proportional to  $(\omega^2 - \Delta^2)^{-1/2}$ . Bardeen explained this situation from the theoretical point of view by suggesting his tunnel-Hamiltonian method and speculating that the Cooper-pairing correlations die out inside the barrier, whereas the single-particle densities of states are renormalized by superconductivity [112]. Bardeen's insight proved to be qualitatively valid and even quantitatively correct for quasiparticle currents. At the same time, it failed when Bardeen objected [113] to the possibility of the Josephson coherent tunneling between superconductors [114,115]. Hence, superconducting correlations should preserve, although being weakened, inside the hostile insulating or normal-metal environment.

Peierls [116] and excitonic [117] insulators, as well as any other completely or partially CDW-gapped systems, are a consequence of the electron-hole many-body correlations. The latter, physically and mathematically, are very similar (although not identical!) to superconducting ones. Hence, their manifestations in the quasiparticle currents should also be similar. In this sense, the CDW gaps  $\Sigma$  behave differently from the band gaps  $E_G$  in Esaki diodes. They appear in the  $J(V)$ -dependence and its derivatives as conspicuous features [63–65].

#### 4. Account of inhomogeneity

It is well-known that the dependence of the quasiparticle tunnel current  $J$  on the bias voltage  $V$  across the junction is much less informative than the same dependence of the tunnel conductance  $G = dJ/dV$ , the CVC. Technically, the latter is determined as the ratio  $\Delta J/\Delta V$ , where  $\Delta J$  is the increment of the current between two voltage values separated by  $\Delta V$ . Plenty of experiments for various solids testify that, if  $\Delta V$  is small enough, the ratio  $\Delta J/\Delta V$  calculated from the data adequately reproduces the theoretically expected  $dJ/dV$  even if the latter contains such peculiarities as jumps, cusps, and so on [99,115]. Nevertheless, if we tried to use the formulas of Section 3 (see relevant calculations in Ref. 30) for the comparison with  $G(V)$ -dependences actually measured for symmetric or non-symmetric junctions involving high- $T_c$  oxides, the result would be discouraging.

The key origin of this discrepancy consists in that high- $T_c$  oxides, even single crystal samples, are intrinsically inhomogeneous objects [51]. The most compelling origin of this inhomogeneity is the non-uniform distribution of

oxygen atoms in those non-stoichiometric materials. However, the inhomogeneity may be traced to other causes of the nanoscale phase separation observed not only in superconducting and magnetic oxides [33–37,118,119] but also in other magnets [120,121], non-equilibrium alloys [122], porous systems [123,124], and colloids [125,126].

In the case of STM spectroscopy, the tunnel current is apparently harvested from a small area of the atomic size on the substrate [127]. If the substrate metal is in the normal state, this is really the case. However, if the substrate is a superconductor, the electron properties of the patch under the tip are formed by many-body correlations extending over a linear distance of about the Pippard-BCS coherence length  $\xi_0$  [128]. If electron-hole (CDW) pairing [129,130] is also present, the corresponding correlation length is of importance as well. The both lengths, although reduced owing to defects, may be much larger than the lattice constants [131]. In other words, the measured quasiparticle tunnel current is actually averaged over rather a large region of the electrode surface. Nevertheless, while scanning along the sample surfaces of various cuprates, the measured CVCs change appreciably [34,39–49,55], which brings us to a conclusion that SCDWs are really electronically inhomogeneous objects characterized by certain distributions of their parameters. As a result, the calculation of the tunnel current should include averaging over those distributions. Since we calculate CVCs for a fixed tip position over the oxide surface, the chosen distribution is considered as a characteristics of this position. Another location of the tip may reveal a different distribution, in accordance with the experiment.

In our previous calculations [60], we showed that taking the spread of only one of SCDW parameters into account (in the case concerned, it was the parameter  $\Sigma_0$ ) was not sufficient to reproduce the quasiparticle CVCs for non-symmetric junctions with SCDWs. In this work, we let all SCDW initial parameters  $X = (\Delta_0, \Sigma_0, \alpha)$  vary. We assumed that the distribution for each of them is described by the bell-shaped function  $w(X)$  proportional to  $\delta_{\geq P_0}^{-4} ((X - X_0)^2 - \delta_{\geq P_0}^2)^2$  within the corresponding intervals  $[X_0 - \delta_{< X_0}, X_0]$  and  $[X_0, X_0 + \delta_{> X_0}]$ , equal to zero outside them, and with the unity normalization in the interval  $Z(X_0) = [X_0 - \delta_{< X_0}, X_0 + \delta_{> X_0}]$ . Below, for brief, we mark this distribution as  $(X_0)_{-\delta_{< P_0}}^{+\delta_{> P_0}}$ .

The procedure of finding  $G$  at the bias voltage  $V$  was as follows. First, we calculated the normalized average currents  $\langle j \rangle$  at the voltages  $V - \Delta V$  and  $V + \Delta V$ . The voltage increment  $\Delta V$  was selected small enough for the final result not to depend on it. Each averaged current  $\langle j(V \pm \Delta V) \rangle$  was calculated as the weighted integral

$$\langle j(V) \rangle = \int j(X, V) w(\Delta_0) w(\Sigma_0) w(\alpha) dX, \quad (19)$$

where  $j(X, V)$  is the current  $J(V)$  calculated for the parameter set  $X = (\Delta_0, \Sigma_0, \alpha)$  using formula (16) but without the algebraic multiplier before the integral. It is easy to verify that, with this normalization, the dependence  $\langle j(V) \rangle$  has the Ohmic asymptotics  $\langle j(V \rightarrow \pm\infty) \rangle \rightarrow V$ . Integration was carried out in the parameter region  $Z(\Delta_0) \times Z(\Sigma_0) \times Z(\alpha)$  using the Monte Carlo method. After reaching the required accuracy, the normalized tunnel conductance was found according to the formula

$$g(V) \approx \frac{\langle j(V + \Delta V) \rangle - \langle j(V - \Delta V) \rangle}{2\Delta V}. \quad (20)$$

The results of calculations (see Sec. 6) showed that the relevant experimental CVCs better correspond to small  $\alpha$ -values. In this case, the variation of  $\alpha$  (also in narrow limits!) gave rise to small CVC changes. Therefore, we selected  $\alpha$  to be a fixed parameter. This choice corresponds to putting  $w(\alpha) = \delta(\alpha - \alpha_0)$  in Eq. (19), and the averaging integration was carried out in the parameter region  $Z(\Delta_0) \times Z(\Sigma_0)$ .

## 5. Conductance-voltage characteristics. Background problem

The electric conductance in tunnel structures is a complex phenomenon including many-body (dynamic electron-plasmon) interactions [132–134]. In the entire voltage range between the Ohmic and Fowler–Nordheim limits, it demonstrates both universal features [135–138] and material-dependent peculiarities [139, 140]. In the case of high- $T_c$  oxides, the CVC behavior is even more involved. For instance, the CVCs often include a background, linear and even asymmetric, which extends over hundreds of millivolts [141, 142]. The origin of this phenomenon has not been clearly identified, so that the exact form of this contribution remains still unknown for both symmetric and non-symmetric junctions with high- $T_c$  oxide SCDWs [141–145]. Moreover, the background component depends not only on the measurement set-up, but also on the studied specimen (see, e.g., measurements [146–149]). Relevant information is too scarce for definite conclusions and assumptions to be made. Let us consider this problem in brief using, in particular, the data of publications [146–149].

The authors of Ref. 149, while studying under- and overdoped Bi2212 oxides, assumed that the measured tunnel current consisted of a true gap-dependent component and a background, the latter being provided by the specimen itself and the measuring equipment. This background was found to vary from one specimen to another, which is quite reasonable, but it was supposed to be independent of the temperature for the fixed combination “specimen + measurement unit”. Therefore, by assuming that the specimen is a normal metal at  $T > T_c$ , the background cur-

rent (more precisely, the background CVC) was measured at those temperatures. Then, the “genuine” CVC was calculated by subtracting this reference CVC from the measured one. However, we know that, at temperatures above  $T_c$ , CVCs for high- $T_c$  oxides demonstrate a pseudogap behavior, which survives up to temperatures much higher than  $T_c$  [31]. At the same time, the presented CVCs, including the reference one, also include a background contribution. It is so because, in the absence of background signal, (i) the measured CVCs have to approach the normalized Ohmic asymptotic  $g_{\text{Ohmic}}(eV) = 1$  at high, by magnitude, bias voltages, and (ii) they must satisfy the “sum rule”: the summed up areas between the plots of a specific CVC and its Ohmic asymptotic to the both sides from the latter must compensate each other. The “sum rule” is known to be dictated by the conservation law for the number of quasiparticle states in the semiconducting model of BCS superconductors [66]. It has to be strictly obeyed for the exact junction conductance. The experimental determination of the latter would require current measurements at two infinitesimally close bias voltages, which is, of course, practically impossible. Nevertheless, we believe that, if the tunnel conductance is calculated as a finite difference across a sufficiently short bias voltage interval, the “sum rule” remains a good criterion for the absence of any background signal in the CVC.

Unfortunately, the majority of experimental CVCs, including those in measurements [146–149], do not satisfy any of those requirements. Attempts to fulfill condition (i) by taking a simple smooth curve with its high-voltage asymptotics repeating those of the specific CVC resulted in the violation of condition (ii). Therefore, the true background is a more complicated function. Now, we have no information on what model should be used in fitting. Moreover, the change of the sought background voltage dependence can strongly affect the resulting “genuine” CVC, which makes the whole problem of the background current determination a non-trivial task.

Taking all the aforesaid into account and bearing in mind the qualitative character of the current analysis, we selected a few CVCs presented in the literature, the background of which can be modeled by a single smooth curve  $g_{\text{bk}}(v)$  satisfying conditions (i) and (ii). This curve had prescribed high- $v$  linear asymptotics with a smooth transition between them:

$$g_{\text{bk}}(v) = \frac{1}{2} \left[ A(-\infty, v) \left( 1 - \tanh \frac{v}{X} \right) + A(+\infty, v) \left( 1 + \tanh \frac{v}{X} \right) \right], \quad (21)$$

where

$$A(s, v) = B_s v + C_s \quad (22)$$

is the linear asymptotic at  $v \rightarrow s$ , the parameter  $s = \pm\infty$  identifies the corresponding asymptotic, and the parameter  $X > 0$  determines the transition interval between two

asymptotics. The procedure of finding  $g_{\text{bk}}(v)$  was nothing else but an attempt to approximate the given CVC by dependence (21). At every fitting routine, the fixed asymptotic parameters  $B_s$  and  $C_s$  were selected on the basis of some reasonable considerations concerning the behavior of analyzed CVC. The fitting procedure was performed using the software package Origin 2016. For plenty of examined CVCs, the resulting  $X$ -values turned out too small. This result meant that either the transition interval was exclusively narrow or, more probably, the selected function  $g_{\text{bk}}(v)$  with prescribed asymptotics did not satisfy condition (ii). In both cases, such CVCs were rejected from further consideration.

## 6. Results of calculations and discussion

Guided by the considerations outlined in Sec. 5, we made attempts to fit  $G(V)$  for high- $T_c$  oxides  $\text{YBa}_2\text{Cu}_3\text{O}_{7-\delta}$  with  $T_c \approx 90$  K (Ref. 148) and  $\text{Bi}_2\text{Sr}_2\text{CaCu}_2\text{O}_{8+\delta}$  with  $T_c \approx 92$  K (Ref. 146). In the both cases, the experimental measurements were carried out at the temperature of  $T = 4.2$  K, so that  $T \ll T_c$ . Therefore, our specific calculations were performed for the temperature  $T = 0$  K. The relevant experimental data together with model background (21), the “true” CVCs, and their fitting curves are shown in Figs. 3 and 4, respectively. As one can see, the main features of the experimental CVCs are reproduced very well in the former case. Specifically, these are (i) the  $d$ -wave-like character of the region between the  $\Delta$ -gap

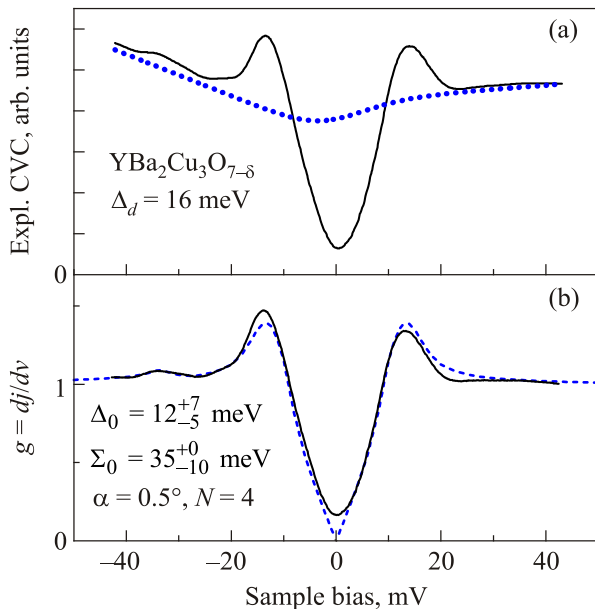


Fig. 3. (Color online) (a) Experimental current-voltage characteristic (CVC) for  $\text{YBa}_2\text{Cu}_3\text{O}_{7-\delta}$  [148] (solid curve) and its assumed background component (dotted curve). (b) Normalized background-free CVC (solid curve) and its fitting in the framework of SCDW model (dashed curve); the corresponding fitting parameters are indicated.

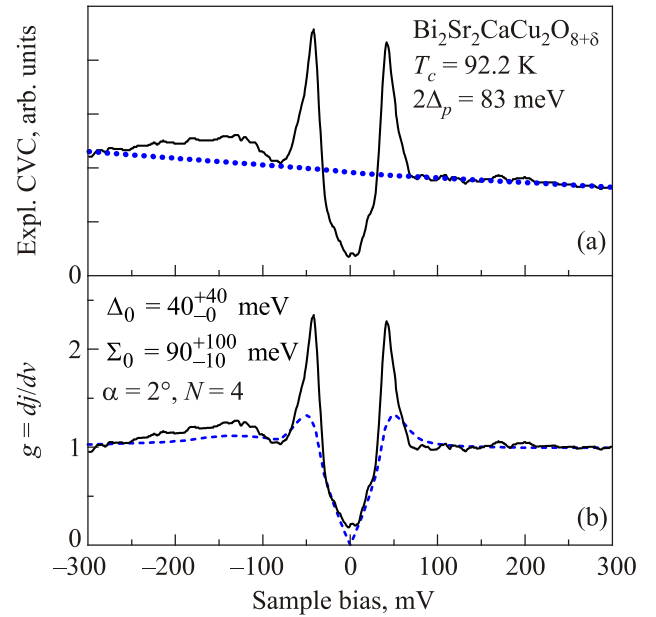


Fig. 4. (Color online) The same as in Fig. 3, but for BSCCO [146].

edges; (ii) the asymmetry of the CVCs with reference to the voltage; and (iii) the dip-hump structure outside the  $d$ -wave gap region. We should mention that the appearance of this structure in the negative-voltage CVC branch corresponds to the selection  $\cos \varphi = -1$  or  $\varphi = \pi$  for the CDW phase (see Sec. 2). One should note that, in the framework of the suggested theory, a slight asymmetry between the inner peaks, which is also typical of the overwhelming majority of experimental CVCs, can also be explained, in addition to the influence of unknown background current, by a slight deviation of the CDW phase from this value (see the relevant discussion in Ref. 106).

At the same time, Fig. 4 demonstrates the importance of the background choice in accordance with the “sum rule” for the density of states. An unsatisfactory selection resulted in that we did not succeed in reproducing the magnitudes of the peaks and humps precisely. We think that the ambiguity of the background account is to blame for this shortcoming. It is worth noticing that various kinds of the quite reasonable normalization intended to exclude the background influence cannot solve this problem (see, e.g., Ref. 39). However, even the CVC shown in Fig. 4 can qualitatively be understood as a consequence of a competition between the CDWs and superconductivity.

The results obtained demonstrate that the FS dielectrization degree in cuprates is low. Nevertheless, it is sufficient to make the CVCs for non-symmetric junctions also non-symmetric and allow a conclusion about the presence of CDWs in cuprates to be made.

The most frequently expressed alternative viewpoint [150–153] attributes the dip-hump structures observed in cuprates [25,55,56] to the extremely strong-coupling ef-



fects, well-known for other superconductors with high  $T_c$  [56,154]. However, in order to implement corresponding models, which suggest an anomalously strong electron interaction with gluing bosons (these models postulate that Cooper pairing in high- $T_c$  oxides is driven by spin fluctuations [5,155–158]), one should additionally conceive the important role of the Van Hove singularities in the electron spectrum [62,159]. Such a reconstruction of the observed features is, of course, possible. Nevertheless, our interpretation discussed here seems to be more appealing. First, it invokes CDWs, which are real phenomena intrinsic to cuprates. Second, CDW effects in tunneling, if not depressed by disorder, are very strong on their own [30], so one does not need any additional amplification by another cause. Third, we can easily explain the symmetry breaking in CVCs as the direct consequence of the CDW existence due to the role of the normal-anomalous Green's function  $G_{tb}$  [106].

Another interpretation of the dip-hump structures, which has been published recently [160], is based on the existence of the normal layer at the degraded superconductor surface and the appearance of the bound state in this layer. However, the corresponding dip-hump features turned out symmetric with respect to the bias voltage in the non-symmetric tunnel junction geometry, contrary to our results and to the experimental ones.

It is instructive to note that the interpretation of the same phenomena in high- $T_c$  oxides steadily changes with time, highly depending on the dominating viewpoint in the community. For instance, the appearance of extra peaks in point-contact CVCs with  $\text{YBa}_2\text{Cu}_3\text{O}_{7-\delta}$  [161] was attributed to phonon manifestations. Similarly, point-contact and tunnel studies of  $\text{YBa}_2\text{Cu}_3\text{O}_{7-\delta}$  [162] and  $\text{Bi}_2\text{Sr}_2\text{CaCu}_2\text{O}_{8+\delta}$  [163], which revealed sub-gap peculiarities, were also considered as the evidence of the phonon-driven Cooper pairing mechanism, as well as the  $s$ -symmetry of superconducting order parameter. This scientific group adopts the more or less conventional character of superconductivity in cuprates [164].

## 7. Conclusions

In this work, we analyzed the issue about the energy gap scatter in cuprates observed by means of tunnel spectroscopy. We showed that the gap spread is due to the dispersion of both the genuine superconducting gap  $\Delta$  and the competing CDW gap  $\Sigma$ . The non-symmetry of the CVCs and the existence of the peak-dip-hump structures for one voltage polarity are other important features revealed in the experimental data. Using our model of the coexistence between  $d$ -wave superconductivity and CDWs, we calculated tunnel CVCs and fitted experimental data for  $\text{YBa}_2\text{Cu}_3\text{O}_{7-\delta}$  and  $\text{Bi}_2\text{Sr}_2\text{CaCu}_2\text{O}_{8+\delta}$ . The results are satisfactory taking into account the background uncertainty, making the comparison of theoretical and experimental values for the conductance  $G(V)$  ambiguous.

The work was partially supported by the Project No. 24 of the 2015–2017 Scientific Cooperation Agreement between Poland and Ukraine.

1. C.W. Chu, L.Z. Deng, and B. Lv, *Physica C* **514**, 290 (2015).
2. M.L. Kulić, *Phys. Rep.* **338**, 1 (2000).
3. *Superconductivity. Conventional and Unconventional Superconductors*, K.H. Bennemann and J.B. Ketterson (eds.), Springer Verlag, Berlin (2008), Vol. 1.
4. *Superconductivity. Novel Superconductors*, K.H. Bennemann and J.B. Ketterson (eds.), Springer Verlag, Berlin (2008), Vol. 2.
5. N.M. Plakida, *High-Temperature Cuprate Superconductors. Experiment, Theory, and Applications*, Springer Verlag, Berlin (2010).
6. *Superconductivity in New Materials*, Z. Fisk and H.R. Ott (eds.), Elsevier, Amsterdam (2011).
7. A.M. Gabovich and V.I. Kuznetsov, *Eur. J. Phys.* **34**, 371 (2013).
8. G.A.C. Ummarino, in: *Emergent Phenomena in Correlated Matter Modeling and Simulation*, E. Pavarini, E. Koch, and U. Schollwöck (eds.), Forschungszentrum Jülich, Jülich (2013), Vol. 3, p. 13.1.
9. L.F. Mattheiss, E.M. Gyorgy, and D.W. Johnson, *Phys. Rev. B* **37**, 3745 (1988).
10. H. Gou, N. Dubrovinskaia, E. Bykova, A.A. Tsirlin, D. Kasinathan, W. Schnelle, A. Richter, M. Merlini, M. Hanfland, A.M. Abakumov, D. Batuk, G. Van Tendeloo, Y. Nakajima, A.N. Kolmogorov, and L. Dubrovinsky, *Phys. Rev. Lett.* **111**, 157002 (2013).
11. G.W. Webb, F. Marsiglio, and J.E. Hirsch, *Physica C* **514**, 17 (2015).
12. P. Fulde, *Electron Correlations in Molecules and Solids*, Springer Verlag, Berlin (1995).
13. P.J. Hirschfeld, *C. R. Physique* **17**, 197 (2016).
14. A.M. Gabovich, A.I. Voitenko, and M. Ausloos, *Phys. Rep.* **367**, 583 (2002).
15. R.A. Klemm, *Physica C* **514**, 86 (2015).
16. N. Doiron-Leyraud, S. Badoux, S.R. de Cotret, S. Lepault, D. LeBoeuf, F. Laliberté, E. Hassinger, B.J. Ramshaw, D.A. Bonn, W.N. Hardy, R. Liang, J-H. Park, D. Vignolles, B. Vignolle, L. Taillefer, and C. Proust, *Nat. Commun.* **6**, 6034 (2015).
17. R. Comin, R. Sutarto, E.H. da Silva Neto, L. Chauviere, R. Liang, W.N. Hardy, D.A. Bonn, F. He, G.A. Sawatzky, and A. Damascelli, *Science* **347**, 1335 (2015).
18. S.E. Sebastian and C. Proust, *Annu. Rev. Condens. Matter Phys.* **6**, 411 (2015).
19. T. Wu, H. Mayaffre, S. Krämer, M. Horvatić, C. Berthier, W.N. Hardy, R. Liang, D.A. Bonn, and M-H. Julien, *Nat. Commun.* **6**, 6438 (2015).
20. R. Comin, R. Sutarto, F. He, E.H. da Silva Neto, L. Chauviere, A. Frap-C R. Liang, W.N. Hardy, D.A. Bonn, Y. Yoshida, H. Eisaki, A.J. Achkar, D.G. Hawthorn, B. Keimer, G.A. Sawatzky, and A. Damascelli, *Nature Mater.* **14**, 796 (2015).

21. E.M. Forgan, E. Blackburn, A.T. Holmes, A.K.R. Briffa, J. Chang, L. Bouchenoire, S.D. Brown, R. Liang, D. Bonn, W.N. Hardy, N.B. Christensen, M.V. Zimmermann, M. Hücker, and S.M. Hayden, *Nat. Commun.* **5**, 10064 (2015).
22. O. Cyr-Choinière, G. Grissonnanche, S. Badoux, J. Day, D.A. Bonn, W.N. Hardy, R. Liang, N. Doiron-Leyraud, and L. Taillefer, *Phys. Rev. B* **92**, 224502 (2015).
23. S. Gerber, H. Jang, H. Nojiri, S. Matsuzawa, H. Yasumura, D.A. Bonn, R. Liang, W.N. Hardy, Z. Islam, A. Mehta, S. Song, M. Sikorski, D. Stefanescu, Y. Feng, S.A. Kivelson, T.P. Devereaux, Z-X. Shen, C-C. Kao, W-S. Lee, D. Zhu, and J-S. Lee, *Science* **350**, 949 (2015).
24. T. Kurosawa, G. Hatta, H. Miyazaki, J. Yamaji, K. Yoshikawa, Y. Nakagawa, Y. Shibata, H. Yoshida, M. Oda, M. Ido, K. Takeyama, and N. Momono, *Int. J. Mod. Phys. B* **29**, 1542009 (2015).
25. A.M. Gabovich, A.I. Voitenko, T. Ekino, M.S. Li, H. Szymczak, and M. Pękała, *Adv. Condens. Matter Phys.* **2010**, Article ID 681070 (2010).
26. T. Ekino, A.M. Gabovich, M.S. Li, M. Pękała, H. Szymczak, and A.I. Voitenko, *Symmetry* **3**, 699 (2011).
27. T. Ekino, A.M. Gabovich, M.S. Li, M. Pękała, H. Szymczak, and A.I. Voitenko, *J. Phys.: Condens. Matter* **23**, 385701 (2011).
28. A.M. Gabovich and A.I. Voitenko, *Fiz. Nizk. Temp.* **39**, 301 (2013) [*Low Temp. Phys.* **39**, 232 (2013)].
29. M. Hashimoto, I.M. Vishik, R-H. He, T.P. Devereaux, and Z-X. Shen, *Nature Phys.* **10**, 483 (2014).
30. A.M. Gabovich, M.S. Li, H. Szymczak, and A.I. Voitenko, *Phys. Rev. B* **92**, 054512 (2015).
31. A.A. Kordyuk, *Fiz. Nizk. Temp.* **41**, 417 (2015) [*Low Temp. Phys.* **41**, 319 (2015)][].
32. T. Yoshida, W. Malaeb, S. Ideta, D.H. Lu, R.G. Moor, Z-X. Shen, M. Okawa, T. Kiss, K. Ishizaka, S. Shin, S. Komiya, Y. Ando, H. Eisaki, S. Uchida, and A. Fujimori, *Phys. Rev. B* **93**, 014513 (2016).
33. J.C. Phillips, A. Saxena, and A.R. Bishop, *Rep. Prog. Phys.* **66**, 2111 (2003).
34. I. Zeljkovic and J.E. Hoffman, *Phys. Chem. Chem. Phys.* **15**, 13462 (2013).
35. E.W. Carlson, *Nature* **525**, 329 (2015).
36. G. Campi, A. Bianconi, N. Poccia, G. Bianconi, L. Barba, G. Arrighetti, D. Innocenti, J. Karpinski, N.D. Zhigadlo, S.M. Kazakov, M. Burghammer, M. v Zimmermann, M. Sprung, and A. Ricci, *Nature* **525**, 359 (2015).
37. G. Campi and A. Bianconi, *J. Supercond.* **29**, 627 (2016).
38. M.H. Hamidian, S.D. Edkins, C.K. Kim, J.C. Davis, A.P. Mackenzie, H. Eisaki, S. Uchida, M.J. Lawler, E-A. Kim, S. Sachdev, and K. Fujita, *Nature Phys.* **12**, 150 (2016).
39. M.C. Boyer, W.D. Wise, K. Chatterjee, M. Yi, T. Kondo, T. Takeuchi, H. Ikuta, and E.W. Hudson, *Nature Phys.* **3**, 802 (2007).
40. S.H. Pan, J.P. O'Neal, R.L. Badzey, C. Chamon, H. Ding, J.R. Engelbrecht, Z. Wang, H. Eisaki, S. Uchida, A.K. Gupta, K-W. Ng, E.W. Hudson, K.M. Lang, and J.C. Davis, *Nature* **413**, 282 (2001).
41. A. Fang, C. Howald, N. Kaneko, M. Greven, and A. Kapitulnik, *Phys. Rev. B* **70**, 214514 (2004).
42. K.K. Gomes, A.N. Pasupathy, A. Pushp, S. Ono, Y. Ando, and A. Yazdani, *Nature* **447**, 569 (2007).
43. K.K. Gomes, A.N. Pasupathy, A. Pushp, S. Ono, Y. Ando, and A. Yazdani, *Physica C* **460–462**, Part1, 212 (2007).
44. A.N. Pasupathy, A. Pushp, K.K. Gomes, C.V. Parker, J. Wen, Z. Xu, G. Gu, S. Ono, Y. Ando, and A. Yazdani, *Science* **320**, 196 (2008).
45. A. Yazdani, *J. Phys.: Condens. Matter* **21**, 164214 (2009).
46. T. Kato, H. Funahashi, H. Nakamura, M. Fujimoto, T. Machida, H. Sakata, S. Nakao, and T. Hasegawa, *J. Supercond.* **23**, 771 (2010).
47. N. Miyakawa, K. Tokiwa, S. Mikusu, J.F. Zasadzinski, L. Ozyuzer, T. Ishihara, T. Kaneko, T. Watanabe, and K.E. Gray, *Int. J. Mod. Phys. B* **17**, 3612 (2003).
48. A. Sugimoto, T. Ekino, K. Tanaka, K. Mineta, K. Tanabe, and K. Tokiwa, *Phys. Proced.* **58**, 78 (2014).
49. N. Miyakawa, K. Tokiwa, S. Mikusu, T. Watanabe, A. Iyo, J.F. Zasadzinski, and T. Kaneko, *Int. J. Mod. Phys. B* **19**, 225 (2005).
50. A.I. Gusev, *Usp. Fiz. Nauk* **184**, 905 (2014).
51. M. Karppinen and H. Yamauchi, *Mat. Sci. Eng. R* **26**, 51 (1999).
52. H. Hilgenkamp and J. Mannhart, *Rev. Mod. Phys.* **74**, 485 (2002).
53. F. Tafuri, J.R. Kirtley, F. Lombardi, P.G. Medaglia, P. Orgiani, and G. Balestrino, *Fiz. Nizk. Temp.* **30**, 785 (2004). [*Low Temp. Phys.* **30**, 591 (2004)].
54. F. Tafuri and J.R. Kirtley, *Rep. Prog. Phys.* **68**, 2573 (2005).
55. Ø. Fischer, M. Kugler, I. Maggio-Aprile, and C. Berthod, *Rev. Mod. Phys.* **79**, 353 (2007).
56. J.F. Zasadzinski, in: *Superconductivity. Novel Superconductors*, K.H. Bennemann and J.B. Ketterson (eds.), Springer Verlag, Berlin (2008), Vol. 2, p. 833.
57. A.M. Gabovich and A.I. Voitenko, *Phys. Rev. B* **75**, 064516 (2007).
58. T. Ekino, A.M. Gabovich, M.S. Li, M.P. Pękała, H. Szymczak, and A.I. Voitenko, *Phys. Rev. B* **76**, 180503 (2007).
59. T. Ekino, A.M. Gabovich, and A.I. Voitenko, *Fiz. Nizk. Temp.* **34**, 515 (2008) [*Low Temp. Phys.* **34**, 409 (2008)].
60. A.M. Gabovich and A.I. Voitenko, *Physica C* **503**, 7 (2014).
61. A. Damascelli, Z. Hussain, and Z-X. Shen, *Rev. Mod. Phys.* **75**, 473 (2003).
62. T. Das, R.S. Markiewicz, and A. Bansil, *Adv. Phys.* **63**, 151 (2014).
63. R.V. Coleman, B. Giambattista, P.K. Hansma, A. Johnson, W.W. McNairy, and C.G. Slough, *Adv. Phys.* **37**, 559 (1988).
64. B. Giambattista, C.G. Slough, W.W. McNairy, and R.V. Coleman, *Phys. Rev. B* **41**, 10082 (1990).
65. P. Monceau, *Adv. Phys.* **61**, 325 (2012).
66. M. Tinkham, *Introduction to Superconductivity*, Dover, Mineola, NY (2004).
67. T. Ekino, Y. Sezaki, and H. Fujii, *Phys. Rev. B* **60**, 6916 (1999).

68. T. Kurosawa, T. Yoneyama, Y. Takano, M. Hagiwara, R. Inoue, N. Hagiwara, K. Kurusu, K. Takeyama, N. Momono, M. Oda, and M. Ido, *Phys. Rev. B* **81**, 094519 (2010).
69. V.M. Krasnov, A. Yurgens, D. Winkler, P. Delsing, and T. Claeson, *Phys. Rev. Lett.* **84**, 5860 (2000).
70. V.M. Krasnov, A.E. Kovalev, A. Yurgens, and D. Winkler, *Phys. Rev. Lett.* **86**, 2657 (2001).
71. V.N. Zavaritsky, *Phys. Rev. Lett.* **92**, 259701 (2004).
72. N.A. Belous, A.E. Chernyakhovskii, A.M. Gabovich, D.P. Moiseev, and V.M. Postnikov, *J. Phys. C* **21**, L153 (1988).
73. A.J. Berlinsky, *Rep. Prog. Phys.* **42**, 1243 (1979).
74. J.A. Wilson, F.J. Di Salvo, and S. Mahajan, *Adv. Phys.* **24**, 117 (1975).
75. D. Jérôme, C. Berthier, P. Molinié, and J. Rouxel, *J. Phys. (Paris) Colloq.* **37**, C 4, C 125 (1976).
76. D.S. Inosov, V.B. Zabolotnyy, D.V. Evtushinsky, A.A. Kordyuk, B. Büchner, R. Follath, H. Berger, and S.V. Borisenko, *New J. Phys.* **10**, 125027 (2008).
77. A. Sherman and M. Schreiber, *Phys. Rev. B* **77**, 155117 (2008).
78. Y. Wang, D. Chowdhury, and A.V. Chubukov, *Phys. Rev. B* **92**, 161103 (2015).
79. G. Ghiringhelli, M. Le Tacon, M.M.S. Blanco-Canosa, C. Mazzoli, N.B. Brookes, G.M. De Luca, A. Frano, D.G. Hawthorn, F. He, T. Loew, M.M. Sala, D.C. Peets, M. Salluzzo, E. Schierle, R. Sutarto, G.A. Sawatzky, E. Weschke, B. Keimer, and L. Braicovich, *Science* **337**, 821 (2012).
80. Y. Caplan, G. Wachtel, and D. Orgad, *Phys. Rev. B* **92**, 224504 (2015).
81. M. Vojta, *Adv. Phys.* **58**, 699 (2009).
82. R. Daou, J. Chang, D. LeBoeuf, O. Cyr-Choinière, F. Laliberté, N. Doiron-Leyraud, B.J. Ramshaw, R. Liang, D.A. Bonn, W.N. Hardy, and L. Taillefer, *Nature* **463**, 519 (2010).
83. E.H. da Silva Neto, P. Aynajian, R.E. Baumbach, E.D. Bauer, J. Mydosh, S. Ono, and A. Yazdani, *Phys. Rev. B* **87**, 161117 (2013).
84. S. Sugai, Y. Takayanagi, N. Hayamizu, T. Muroi, R. Shiozaki, J. Nohara, K. Takenaka, and K. Okazaki, *J. Phys.: Condens. Matter* **25**, 475701 (2013).
85. Y. Wang and A. Chubukov, *Phys. Rev. B* **90**, 035149 (2014).
86. A.J. Achkar, M. Zwiebler, C. McMahon, F. He, R. Sutarto, I. Djianto, Z. Hao, M.J.P. Gingras, M. Hücker, G.D. Gu, A. Revcolevschi, H. Zhang, Y.-J. Kim, J. Geck, and D.G. Hawthorn, *Science* **351**, 576 (2016).
87. A.M. Gabovich, V.A. Medvedev, D.P. Moiseev, A.A. Motuz, A.F. Prikhot'ko, L.V. Prokopovich, A.V. Solodukhin, L.I. Khirunencko, V.K. Shinkarenko, A.S. Shpigel, and V.E. Yachmenev, *Fiz. Nizk. Temp.*, 844 (1987) [*Low Temp. Phys.* **13**, 483 (1987)].
88. A.M. Gabovich, D.P. Moiseev, A.S. Shpigel, and A.I. Voitenko, *Phys. Status Solidi B* **161**, 293 (1990).
89. A.M. Gabovich, M.S. Li, H. Szymczak, and A.I. Voitenko, *Phys. Rev. B* **87**, 104503 (2013).
90. G. Bilbro and W.L. McMillan, *Phys. Rev. B* **14**, 1887 (1976).
91. A.M. Gabovich, M.S. Li, H. Szymczak, and A.I. Voitenko, *J. Phys.: Condens. Matter* **15**, 2745 (2003).
92. H. Won and K. Maki, *Phys. Rev. B* **49**, 1397 (1994).
93. A. Yurgens, D. Winkler, T. Claeson, S.-J. Hwang, and J.-H. Choy, *Int. J. Mod. Phys. B* **13**, 3758 (1999).
94. V.M. Krasnov, *Phys. Rev. B* **91**, 224508 (2015).
95. Q. Li, Y.N. Tsay, M. Suenaga, R.A. Klemm, G.D. Gu, and N. Koshizuka, *Phys. Rev. Lett.* **83**, 4160 (1999).
96. Y. Takano, T. Hatano, A. Fukuyo, A. Ishii, M. Ohmori, S. Arisawa, K. Togano, and M. Tachiki, *J. Low Temp. Phys.* **131**, 533 (2003).
97. Yu.I. Latyshev, A.P. Orlov, A.M. Nikitina, P. Monceau, and R.A. Klemm, *Phys. Rev. B* **70**, 094517 (2004).
98. R.A. Klemm, *Phil. Mag.* **85**, 801 (2005).
99. A.I. Larkin and Yu. N. Ovchinnikov, *Zh. Éksp. Teor. Fiz.* **51**, 1535 (1966) [*Sov. Phys. JETP* **24**, 1035 (1966)].
100. A.M. Gabovich and A.I. Voitenko, *Phys. Rev. B* **55**, 1081 (1997).
101. A.M. Gabovich and A.I. Voitenko, *J. Phys.: Condens. Matter* **9**, 3901 (1997).
102. A.I. Voitenko and A.M. Gabovich, *Fiz. Tverd. Tela* **49**, 1356 (2007).
103. T. Ekino, A.M. Gabovich, M.S. Li, M. Pękała H. Szymczak, and A.I. Voitenko, *J. Phys.: Condens. Matter* **20**, 425218 (2008).
104. Yu.V. Kopaev, *Trudy Fiz. Inst. Akad. Nauk SSSR* **86**, 3 (1975).
105. A.M. Gabovich, E.A. Pashitskii, and A.S. Shpigel, *Fiz. Tverd. Tela* **18**, 3279 (1976) [*Sov. Phys. Solid State* **18**, 1911 (1976)].
106. A.M. Gabovich and A.I. Voitenko, *Phys. Rev. B* **56**, 7785 (1997).
107. N. Jenkins, Y. Fasano, C. Berthod, I. Maggio-Aprile, A. Piriou, E. Giannini, B.W. Hoogenboom, C. Hess, T. Cren, and Ø. Fischer, *Phys. Rev. Lett.* **103**, 227001 (2009).
108. W.A. Harrison, *Phys. Rev.* **123**, 85 (1961).
109. E.C. Kemble, *The Fundamental Principles of Quantum Mechanics with Elementary Applications*, McGraw-Hill, New York (1937).
110. I. Giaever, *Phys. Rev. Lett.* **5**, 147 (1960).
111. I. Giaever, *Phys. Rev. Lett.* **5**, 464 (1960).
112. J. Bardeen, *Phys. Rev. Lett.* **6**, 57 (1961).
113. J. Bardeen, *Phys. Rev. Lett.* **9**, 147 (1962).
114. B.D. Josephson, *Phys. Lett.* **1**, 251 (1962).
115. A. Barone and G. Paterno, *The Physics and Applications of the Josephson Effect*, John Wiley and Sons, New York (1982).
116. R. Peierls, *Ann. Phys.* **4**, 121 (1930).
117. L.V. Keldysh and Yu.V. Kopaev, *Fiz. Tverd. Tela* **6**, 2791 (1964) [*Sov. Phys. Solid State* **6**, 2219 (1965)].
118. E.L. Nagaev, *Usp. Fiz. Nauk* **165**, 529 (1995) [*Physics Usp.* **38**, 497 (1995)].
119. E. Dagotto, T. Hotta, and A. Moreo, *Phys. Rep.* **344**, 1 (2001).
120. E.L. Nagaev, *Zh. Éksp. Teor. Fiz.* **54**, 228 (1968).
121. M.A. Krivoglaz, *Usp. Fiz. Nauk* **111**, 617 (1973).
122. V.G. Vaks, *Phys. Rep.* **391**, 157 (2004).
123. D.H. Rothman, *Rev. Mod. Phys.* **66**, 1417 (1994).
124. L.D. Gelb, K.E. Gubbins, R. Radhakrishnan, and M. Sliwinska-Bartkowiak, *Rep. Prog. Phys.* **62**, 1573 (1999).

125. P. Koets, *Rep. Prog. Phys.* **10**, 129 (1944).
126. R. Tuinier, J. Rieger, and C.G. de Kruif, *Adv. Colloid Interface Sci.* **103**, 1 (2003).
127. J. Tersoff and D.R. Hamann, *Phys. Rev. B* **31**, 805 (1985).
128. A.A. Abrikosov, *Fundamentals of the Theory of Metals*, North-Holland, Amsterdam (1988).
129. G. Grüner, *Rev. Mod. Phys.* **60**, 1129 (1988).
130. J.N. Crain, A. Kirakosian, K.N. Altmann, C. Bromberger, S.C. Erwin, J.L. McChesney, J-L. Lin, and F.J. Himpsel, *Phys. Rev. Lett.* **90**, 176805 (2003).
131. P.C. Snijders and H.H. Weitering, *Rev. Mod. Phys.* **82**, 307 (2010).
132. E.N. Economou and K.L. Ngai, *Adv. Chem. Phys.* **27**, 265 (1974).
133. P.J. Feibelman, *Progr. Surf. Sci.* **12**, 287 (1982).
134. A.M. Gabovich, V.M. Rozenbaum, and A.I. Voitenko, *Surf. Sci.* **186**, 523 (1987).
135. J. Frenkel, *Phys. Rev.* **36**, 1604 (1930).
136. J.G. Simmons, *J. Appl. Phys.* **34**, 1793 (1963).
137. J.G. Simmons, *J. Appl. Phys.* **34**, 2581 (1963).
138. E.L. Wolf, *Principles of Electron Tunneling Spectroscopy*, Oxford University Press, New York (1985).
139. *Tunneling Spectroscopy. Capabilities, Applications, and New Techniques*, P.K. Hansma (ed.), Plenum Press, New York (1982).
140. *Scanning Tunneling Microscopy I. General Principles and Applications to Clean and Adsorbate-Covered Surfaces*, H-J. Güntherodt and R. Wiesendanger (eds.), Springer Verlag, Berlin (1992).
141. J.R. Kirtley and D.J. Scalapino, *Phys. Rev. Lett.* **65**, 798 (1990).
142. A.M. Cucolo, R. Di Leo, A. Nigro, P. Romano, and M. Carotenuto, *Phys. Rev. B* **49**, 1308 (1994).
143. P.B. Littlewood and C.M. Varma, *Phys. Rev. B* **45**, 12636 (1992).
144. J.R. Kirtley, S. Washburn, and D.J. Scalapino, *Phys. Rev. B* **45**, 336 (1992).
145. M. Grajcar, A. Plecenik, P. Seidel, V. Vojtanik, and K-U. Barholz, *Phys. Rev. B* **55**, 11738 (2015).
146. Ch. Renner, B. Revaz, J.-Y. Genoud, K. Kadowaki, and Ø. Fischer, *Phys. Rev. Lett.* **80**, 149 (1998).
147. L. Ozyuzer, J.F. Zasadzinski, C. Kendziora, and K.E. Gray, *Phys. Rev. B* **61**, 3629 (1999).
148. A. Sharoni, G. Koren, and O. Millo, *Europhys. Lett.* **54**, 675 (2001).
149. A.K. Gupta and K-W. Ng, *Europhys. Lett.* **58**, 878 (2002).
150. A.V. Chubukov and D.K. Morr, *Phys. Rev. Lett.* **81**, 4716 (1998).
151. M. Eschrig and M.R. Norman, *Phys. Rev. Lett.* **85**, 3261 (2000).
152. C. Berthod, *Phys. Rev. B* **82**, 024504 (2010).
153. C. Berthod, Y. Fasano, I. Maggio-Aprile, A. Piriou, E. Giannini, G. Levy de Castro, and Ø. Fischer, *Phys. Rev. B* **88**, 014528 (2013).
154. W.L. McMillan and J.M. Rowell, in: *Superconductivity*, R.D. Parks (ed.), Dekker, New York (1969), Vol. 1, p. 561.
155. D. Manske, *Theory of Unconventional Superconductors. Cooper-Pairing Mediated by Spin Excitations*, Springer Verlag, New York (2004).
156. A.A. Kordyuk and S.V. Borisenko, *Fiz. Nizk. Temp.* **32**, 401 (2006) [*Low Temp. Phys.* **32**, 298 (2006)].
157. P.A. Lee, N. Nagaosa, and X-G. Wen, *Rev. Mod. Phys.* **78**, 17 (2006).
158. D.J. Scalapino, *Rev. Mod. Phys.* **84**, 1383 (2012).
159. R.S. Markiewicz, *J. Phys. Chem. Sol.* **58**, 1179 (1997).
160. E. Zhitlukhina, I. Devyatov, O. Egorov, M. Belogolovskii, and P. Seidel, *Nanoscale Res. Lett.* **11**, 58 (2016).
161. V.M. Dmitriev, A.L. Solovyev, and A.I. Dmitrenko, *Fiz. Nizk. Temp.* **15**, 356 (1989) [*Sov. J. Low Temp. Phys.* **15**, 200 (1989)].
162. Ya.G. Ponomarev, B.A. Aminov, N.B. Brandt, M. Hein, C.S. Khi, V.Z. Kresin, G. Müller, H. Piel, K. Rosner, S.V. Tchesnokov, E.B. Tsokur, D. Wehler, R. Winzer, Th. Wolfe, A.V. Yarygin, and K.T. Yusupov, *Phys. Rev. B* **52**, 1352 (1995).
163. Ya.G. Ponomarev, C.S. Khi, K.K. Uk, M.V. Sudakova, S.N. Tchesnokov, M.A. Lorenz, M.A. Hein, G. Müller, H. Piel, B.A. Aminov, A. Krapf, and W. Kraak, *Physica C* **315**, 85 (1999).
164. Ya.G. Ponomarev and H.H. Van, *Phys. Proceed.* **36**, 611 (2013).